Synthetic Biology and Engineering

SCIEPublish

Communication

Engineering Probiotic *Escherichia coli* Nissle 1917 for 2′-Fucosyllactose and 3-Fucosyllactose Biosynthesis

Meng-Ru Wang [1], Fang-Qi Shao [1], Hong-Zhi Sheng [2], Wei Zhang [2], Yi-Ran Xu [1] and Zheng-Jun Li [1,*]

[1] State Key Laboratory of Green Biomanufacturing, National Energy R&D Center for Biorefinery, and Beijing Key Laboratory of Green Chemicals Biomanufacturing, Beijing University of Chemical Technology, Beijing 100029, China; wangmr@im.ac.cn (M.-R.W.); 2026400236@buct.edu.cn (F.-Q.S.); 2023090056@buct.edu.cn (Y.-R.X.)

[2] Deep Sea Biology (Shenzhen) Co., Ltd., Shenzhen 518071, China; shz@deepseabio.com (H.-Z.S.); zhangwei@deepseabio.com (W.Z.)

* Corresponding author. E-mail: lizj@mail.buct.edu.cn (Z.-J.L.)

Received: 4 August 2026; Revised: 31 August 2026; Accepted: 17 September 2026; Available online: 20 September 2026

ABSTRACT: Fucosylated human milk oligosaccharides are valuable targets for microbial biomanufacturing. Here we engineered the probiotic *Escherichia coli* Nissle 1917 as a versatile chassis for synthesizing both 2′-fucosyllactose and 3-fucosyllactose. We implemented lactose preservation and blocked colanic acid precursor consumption while reinforcing the *de novo* GDP-L-fucose pathway. This core module was coupled with either WbgL or FutM2 to drive terminal fucosylation. Initial screening yielded a 2′-fucosyllactose titer of approximately 1.21 g/L. Integrating an additional chromosomal *wbgL* cassette increased the titer to approximately 1.58 g/L, whereas subsequent genomic modifications did not further improve the 2′-FL titer. Cultivation with 30 g/L glycerol and 5 g/L yeast extract significantly improved productivity, enabling the strain to produce approximately 7.71 g/L of 2′-fucosyllactose in shake-flask cultures. Conversely, the FutM2 strain produced 0.38 g/L 3-fucosyllactose without yeast extract and nutrient supplementation unexpectedly suppressed product accumulation despite promoting biomass formation. The work provides a probiotic-chassis proof of concept and identifies product-module physiology as a priority for further engineering.

Keywords: Nissle 1917; 2′-Fucosyllactose; 3-Fucosyllactose; GDP-L-fucose; Probiotic chassis

1. Introduction

Human milk oligosaccharides (HMOs) are unconjugated glycans that shape interactions among diet, the infant microbiota, intestinal epithelia, and immunity. Most HMOs contain lactose at the reducing end and are extended or decorated with fucose or sialic acid. Among the fucosylated structures, 2′-fucosyllactose (2′-FL) and its positional isomer 3-fucosyllactose (3-FL) have emerged as prominent targets for both nutritional research and industrial biomanufacturing. They share the same precursors, specifically lactose and GDP-L-fucose, but require distinct terminal fucosyltransferases. Therefore, 2′-FL and 3-FL

© 2026 The authors. This is an open access article under the Creative Commons Attribution 4.0 International License (https://creativecommons.org/licenses/by/4.0/).

serve as a highly useful pair for probing which metabolic limitations are inherent to the common donor pathway and which are strictly product specific [1–4].

Currently, HMO production is no longer restricted to conventional *Escherichia coli* hosts. Engineered plants have provided a photosynthetic route to multiple HMO structures, while *Corynebacterium glutamicum* and *Bacillus subtilis* have been developed as alternative microbial hosts for *de novo* 2′-FL synthesis. In parallel, synthetic biology is expanding toward sialylated and more structurally complex HMOs [5–8]. The diversification of these production platforms broadens the evaluation criteria for an optimal HMO cell factory. While volumetric titer remains a primary metric, factors such as feedstock utilization, genetic stability, product selectivity, host safety, and compatibility with downstream purification increasingly determine the practical value of the platform.

In *E. coli*, the production of 2′-FL has been significantly improved through strategies that prevent lactose degradation, reinforce the *de novo* or salvage GDP-L-fucose pathways, balance cofactor and precursor supplies, integrate pathway genes into the chromosome, and screen for highly active α1,2-fucosyltransferases [9–15]. While this modular logic has also been applied to 3-FL synthesis, α1,3-fucosyltransferase activity frequently remains a rate limiting bottleneck. FutM2 and other α1,3-fucosyltransferases have therefore been subjected to enzyme engineering, copy-number optimization, fusion strategies, and plasmid-free pathway construction [16–20]. Recent HMO biosynthesis studies have continued to improve productivity, identify new fucosyltransferases, and diversify carbon-source utilization [21–23].

Notably, most high performing fucosyllactose strains to date are derived from laboratory lineages such as *E. coli* BL21(DE3) or MG1655. By contrast, *E. coli* Nissle 1917 (EcN) is a well-characterized probiotic with a long history of human use [24]. Beyond its probiotic status, this strain differs from conventional laboratory hosts in its native K5 capsular polysaccharide biosynthesis and nutrient specific Csr control of central carbon metabolism [25,26]. EcN is also an established chassis for living diagnostics and therapeutics, including engineered strains that sense intestinal inflammation or remove disease-associated metabolites [27,28]. Recent work on navigable genome engineering and biocontainment further illustrates how probiotic chassis can be developed systematically and safely [29,30]. This host is therefore scientifically interesting for HMO synthesis because it tests pathway portability in a physiologically distinct background.

In this study, we engineered EcN as a parallel platform for 2′-FL and 3-FL production by coupling a shared *de novo* GDP-L-fucose module with either WbgL or FutM2 terminal fucosylation. We systematically evaluated effective metabolic interventions and determined the cross-pathway transferability of optimized culture conditions. This design enables a direct comparison between shared host constraints and product specific limitations within the exact same probiotic chassis.

2. Materials and Methods

2.1. Strains, Plasmids, and Pathway Organization

The bacterial strains and plasmids used in this study are listed in Table 1. *E. coli* Nissle 1917 (EcN) was the parental probiotic chassis, *E. coli* MG1655 was used for cloning or as a source of pathway genes, and *E. coli* S17-1 served as the conjugative donor for introducing suicide and genome-editing plasmids into EcN. Oligonucleotides were synthesized by BGI Genomics (Beijing, China) and are listed in Tables S1 and S2.

The codon-optimized α1,2-fucosyltransferase gene *wbgL* from *E. coli* O126 (GenBank AY849806.1) was synthesized by BGI Genomics and amplified with primers *wbgL*-F/R. The *rcsA* and *rcsB* genes were amplified from *E. coli* MG1655 with primers *rcsA*-F/R and *rcsB*-F/R, respectively. The *rcsA* and *rcsB* genes encode positive transcriptional regulators of the colanic acid operon, and their co-overexpression activates the endogenous promoter driving the *manC-manB* and *gmd-wcaG* cluster, thereby reinforcing metabolic flux through the GDP-L-fucose biosynthetic pathway. These three inserts and the pETDuet-1 backbone amplified with V3-F/R were joined using a Gibson Assembly Kit (Vazyme Biotech, Nanjing, China),

placing *rcsA-rcsB* in MCS1 and *wbgL* in MCS2 to generate pET-ABW. For the 3-FL module, a codon-optimized *futM2* gene from *Bacteroides gallinaceum* (GenBank WP_204430034.1) was synthesized and amplified with FutM2-F/R. The pET-ABW-derived backbone was amplified with V5-F/R, and the two fragments were assembled to replace *wbgL* with *futM2*, generating pET-ABF. The *manC-manB* and *gmd-wcaG* clusters were inserted into MCS1 and MCS2 of pRSFDuet-1, respectively, to generate pRSF-CBGW. All Gibson assemblies were performed according to the manufacturer's instructions, and the recombinant plasmids were verified by DNA sequencing.

Table 1. Strains and plasmids used in this study.

Item	Relevant Characteristics	Source
E. coli MG1655	Wild-type for gene cloning	Laboratory stock
EcN	Wild-type *Escherichia coli* Nissle 1917	Laboratory stock
EcN(DE3)	EcN carrying the DE3 expression element	This study
7ZJ	EcN(DE3) Δ*lacZ* Δ*wcaJ*	This study
7ZJW	7ZJ Δ*lacZ*Δ*wcaJ*Δ*lldD*::P_{J23119}-*wbgL*	This study
7ZJWP	7ZJW with the native *manC* promoter replaced by P1	This study
7ZJWPN	7ZJWP Δ*nudD*	This study
7ZJ-2FL	7ZJ harboring pRSF-CBGW and pET-ABW	This study
7ZJW-2FL	7ZJW harboring pRSF-CBGW and pET-ABW	This study
7ZJWP-2FL	7ZJWP harboring pRSF-CBGW and pET-ABW	This study
7ZJWPN-2FL	7ZJWPN harboring pRSF-CBGW and pET-ABW	This study
7ZJ-3FL	7ZJ harboring pRSF-CBGW and pET-ABF	This study
pRSF-CBGW	pRSFDuet-1 derivative; *manC-manB* in MCS1 and *gmd-wcaG* in MCS2	This study
pET-ABW	pETDuet-1 derivative; *rcsA-rcsB* in MCS1 and *wbgL* in MCS2	This study
pET-ABF	pETDuet-1 derivative; *rcsA-rcsB* in MCS1 and *futM2* in MCS2	This study
pRE112-wbgL	pRE112 with gene *wbgL*	This study
pRE112-P1	pRE112 with promoter P1	This study
pRE112-DE3	pRE112 with DE3 fragment	This study

2.2. Construction of Engineered EcN Strains

Because wild-type EcN lacks a T7 RNA polymerase expression system, the DE3 fragment was integrated into its chromosome by pRE112-mediated homologous recombination, replacing *poxB* and generating EcN(DE3). The suicide plasmid was transferred from *E. coli* S17-1 by conjugation. The *lacZ* and *wcaJ* genes were then inactivated by introducing premature stop codons using a CRISPR/nCas9 cytosine base-editing system, thereby generating the basal chassis 7ZJ. Inactivation of *lacZ* was intended to preserve lactose, whereas inactivation of *wcaJ* was intended to reduce diversion of GDP-L-fucose into colanic-acid biosynthesis.

For additional 2′-FL pathway engineering, the *lldD* coding region in 7ZJ was replaced with a P_{J23119}-*wbgL* cassette to generate 7ZJW. The production strain 7ZJW-2FL retained pET-ABW, so chromosomal *wbgL* increased total gene dosage rather than replacing plasmid expression. The native *manC* promoter was subsequently replaced with the stronger P1 promoter to generate 7ZJWP. Finally, *nudD*, which encodes a GDP-mannose hydrolase, was inactivated by base editing to generate 7ZJWPN and reduce loss of the GDP-L-fucose precursor GDP-mannose. Chromosomal replacements were mediated with pRE112 derivatives. All engineered loci were screened by colony PCR and verified by DNA sequencing.

2.3. Media and Culture Conditions

LB, defined medium (DM), minimal medium (MM), mineral salts (MS), M9 medium, and R medium were evaluated. LB contained 10 g/L tryptone, 5 g/L yeast extract, and 10 g/L NaCl. DM contained 20 g/L

glycerol, 13.5 g/L KH_2PO_4, 4.0 g/L $(NH_4)_2HPO_4$, 1.7 g/L citric acid, 1.4 g/L $MgSO_4 \cdot 7H_2O$, and 10 mL/L trace-element solution. The trace-element solution contained 10 g/L Fe(III) citrate, 2.25 g/L $ZnSO_4 \cdot 7H_2O$, 1.0 g/L $CuSO_4 \cdot 5H_2O$, 0.35 g/L $MnSO_4 \cdot H_2O$, 0.23 g/L $Na_2B_4O_7 \cdot 10H_2O$, 0.11 g/L $(NH_4)_6Mo_7O_{24}$, and 2.0 g/L $CaCl_2 \cdot 2H_2O$. MM, MS, M9, and R media were prepared as previously described [31–33].

The pH of each basal medium was adjusted to 6.8 before autoclaving at 115 °C for 30 min. When required, antibiotics were used at final concentrations of 100 µg/mL ampicillin, 50 µg/mL kanamycin, 25 µg/mL chloramphenicol, and 50 µg/mL spectinomycin. To balance enzyme expression with cellular metabolic burden, induction temperatures (25 °C *vs.* 30 °C) and IPTG concentrations (0.1–2.0 mM) were evaluated. Baffled flasks were used for high-oxygen conditions (H), whereas round-bottom flasks were used for low-oxygen conditions (L).

For standard 2′-FL or 3-FL production, a 4-mL LB seed culture was grown at 37 °C and 200 rpm for 12 h. The production culture was inoculated at 2% (*v*/*v*) into 100 mL medium in a 500-mL Erlenmeyer flask. At OD_{600} 0.6–0.8, IPTG and lactose were added, and cultivation continued at 25 °C and 200 rpm for 72 h. For the yeast-extract comparison, the glycerol concentration was increased to 30 g/L, and cultures were prepared either without supplementation or with 5 g/L yeast extract; samples were collected at 0, 24, 48, and 72 h.

2.4. Analytical Methods

Cell growth was monitored spectrophotometrically as OD_{600}. For extracellular metabolite analysis, 1 mL of fermentation broth was centrifuged at 12,000 rpm for 10 min, and the supernatant was passed through a 0.22-µm membrane filter. Concentrations of 2′-FL, 3-FL, lactose, and glycerol were determined using a Shimadzu LC-20A HPLC system (Shimadzu, Kyoto, Japan) fitted with a Bio-Rad Aminex HPX-87H organic-acid column. The mobile phase was 5 mM H_2SO_4 at 0.6 mL/min; the column was maintained at 55 °C, and the injection volume was 10 µL. All experiments were performed in triplicate, and data are presented as mean ± standard deviation (SD).

3. Results and Discussion

3.1. A Shared EcN Donor Pathway Enabled Product Switching at the Terminal Reaction

The engineering design connected glycerol metabolism to the *de novo* GDP-L-fucose pathway through ManA, ManB, ManC, Gmd, and WcaG (Figure 1). Inactivation of *lacZ* preserved lactose as the acceptor, while *wcaJ* inactivation was intended to reduce competing precursor consumption. The pRSF-CBGW donor module was paired with WbgL for α1,2-fucosylation or FutM2 for α1,3-fucosylation (Table 1). Both strains 7ZJ-2FL and 7ZJ-3FL produced the product assigned in the supplied chromatographic records, showing that EcN supported donor formation and that exchanging the terminal enzyme switched the fucosyllactose regioisomer.

This outcome serves as a fundamental proof of concept for transferring the HMO pathway into a probiotic chassis. Although the individual pathway modules have been implemented previously in laboratory lineages of *E. coli* [4,9–15], their robust operation in EcN cannot be automatically assumed. Inherent variations in promoter output, plasmid maintenance, envelope physiology, and global metabolic regulation exist among distinct strain backgrounds. Utilizing a shared host and donor module for both target molecules establishes a controlled internal comparator. Consequently, performance discrepancies observed between the WbgL and FutM2 systems are unlikely to stem from variations in upstream donor supply and are instead attributable to the terminal module or its specific interaction with host physiology.

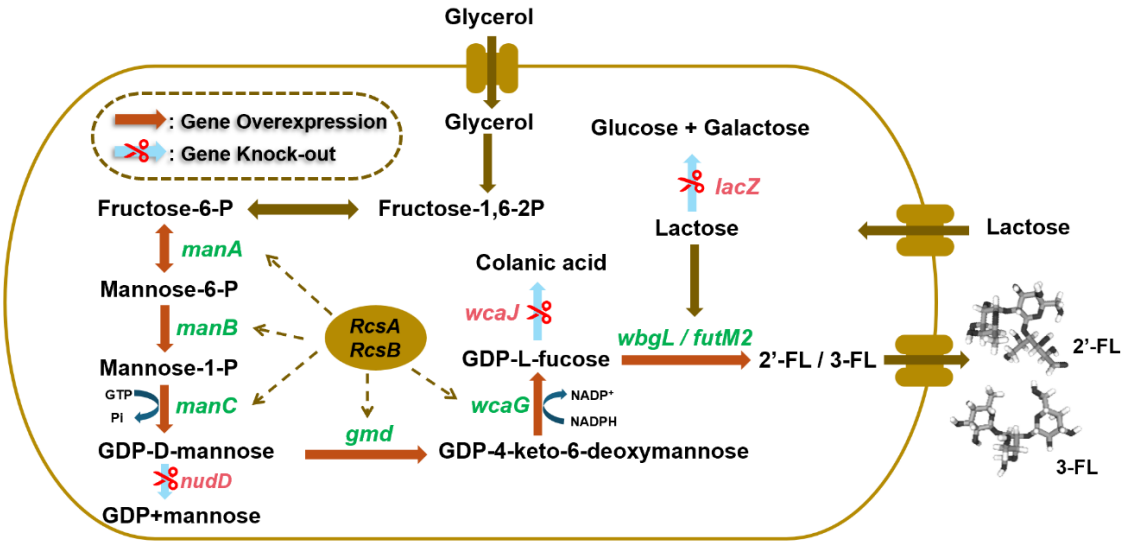

Figure 1. Engineering strategy for 2′-FL and 3-FL biosynthesis in EcN. Glycerol supplies central-carbon intermediates for the ManA–ManB–ManC–Gmd–WcaG *de novo* GDP-L-fucose pathway. Lactose is preserved by *lacZ* inactivation, and *wcaJ* inactivation reduces the diversion of precursor to colanic acid. WbgL and FutM2 catalyze terminal α1,2- and α1,3-fucosylation, respectively. Orange arrows indicate pathway reinforcement; blue arrows with scissors indicate gene inactivation; dashed arrows indicate positive transcriptional activation by RcsA/RcsB.

3.2. Media Formulations Decoupled Biomass Formation from 2′-FL Synthesis

Cultivation across six distinct media revealed an inverse relationship between cell growth and target product accumulation (Figure 2A). Rich LB medium yielded the highest endpoint biomass, reaching OD_{600} of approximately 14.5 at 48 h. In contrast, defined medium (DM) yielded a lower cell density, leveling off near an OD_{600} 10–11 at 36 h. Product formation did not follow this biomass ranking (Figure 2B). DM supported the highest 2′-FL concentration at approximately 1.21 g/L, whereas LB produced only 0.16 g/L while retaining the highest concentration of unreacted lactose. Intermediate titers of 0.44, 0.56, 0.67, and 0.88 g/L were observed in MM, MS, M9, and R media, respectively. DM was therefore identified as the optimal medium because it maximized product concentration rather than total cell mass.

This observed decoupling between biomass formation and product synthesis highlights a fundamental trade off in resource allocation. In LB media, abundant exogenous amino acids and peptide precursors likely relieve anabolic constraints and drive rapid carbon utilization primarily toward building structural macromolecules. We hypothesize that this accelerated cell proliferation competes with heterologous pathway expression by reducing the metabolic availability of cofactors and precursors, which are necessary for GDP-L-fucose synthesis. Furthermore, the elevated residual lactose observed in LB indicates that lactose internalization or downstream glycosylation becomes kinetically uncoupled from rapid growth. Conversely, defined minimal media impose controlled nutrient constraints that moderate specific growth rates. This moderated growth velocity may establish a balanced intracellular regime in which intermediate glycerol flux can be redirected to downstream nucleotide sugars without being cannibalized by rapid biomass synthesis. These findings confirm that maximizing cell density alone does not linearly correlate with high oligosaccharide titers, and optimizing product formation likely requires a controlled growth dynamic to balance energy allocation.

To optimize the T7 expression cascade, we evaluated induction temperatures of 25 °C and 30 °C across an initial IPTG gradient from 0.5 to 2.0 mM (Figure 2C), followed by a finer screen from 0.1 to 0.5 mM at 25 °C (Figure 2D). The combination of 25 °C and 0.5 mM IPTG was selected for subsequent experiments because it produced the highest observed 2′-FL titer of approximately 1.21 g/L. Elevating the temperature

to 30 °C or increasing the IPTG concentration beyond 0.5 mM led to a decline in 2′-FL accumulation. We present this lower temperature and moderate induction strategy as a plausible approach to balance enzyme expression against excessive metabolic burden. Additionally, varying dissolved oxygen levels during shake flask cultivation had no significant impact on the product titer when tested across 0.1 to 0.5 mM IPTG at 25 °C.

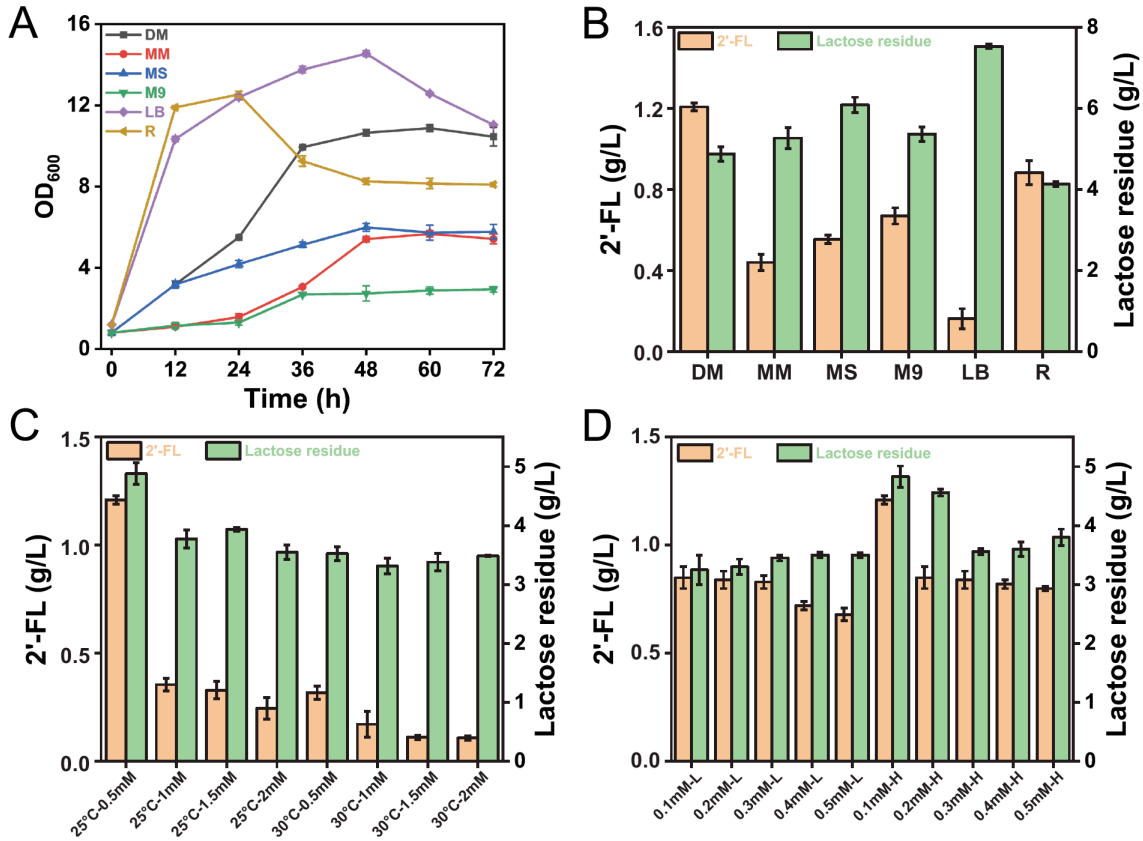

Figure 2. Medium and induction screening for 2′-FL production by 7ZJ-2FL. (**A**) Growth in DM, MM, MS, M9, LB, and R media. (**B**) 2′-FL titer and residual lactose in the six media. (**C**) Effects of induction temperature and IPTG concentration. (**D**) Effects of varying IPTG concentrations and dissolved oxygen levels. L indicates low dissolved oxygen, and H indicates high dissolved oxygen.

3.3. Increasing wbgL Gene Dosage Elevated 2′-FL Titers Prior to Pathway Saturation

The baseline strain 7ZJ-2FL achieved a 2′-FL titer of approximately 1.21 g/L. Integration of a single chromosomal copy of *wbgL* driven by the PJ23119 promoter (strain 7ZJW-2FL) increased the titer to approximately 1.58 g/L, representing a descriptive gain of roughly 31% (Figure 3) with minimal change in residual lactose. Subsequent genomic modifications, including replacing the native *manC* promoter with P1T and inactivating *nudD*, resulted in titers of approximately 1.56 and 1.57 g/L, respectively. These subsequent modifications indicate a clear performance plateau rather than further enhancement.

The initial gain in titer indicates that alpha 1,2 fucosyltransferase capacity was a primary bottleneck in the baseline strain and that increasing terminal enzyme dosage relieved part of this constraint. This finding aligns with previous studies emphasizing the rate limiting nature of fucosyltransferase activity and solubility in heterologous synthesis systems [9,13,21,22]. However, because strain 7ZJW-2FL retained the expression plasmid, this experiment demonstrates a positive dosage response rather than the complete substitution of plasmid-based expression. The lack of further performance gains following *manC* promoter replacement or *nudD* deletion suggests that GDP-mannose synthesis and hydrolysis were not limiting under the evaluated conditions. It is plausible that metabolic flux became constrained by downstream reactions.

The system may also be limited by intracellular cofactor regeneration, specifically the availability of GTP and NADPH. Furthermore, cumulative genomic alterations might have imposed an unanticipated cellular burden. We emphasize that these potential mechanisms remain working hypotheses. Direct quantification of intracellular nucleotide sugar pools and specific enzyme activities will be required to pinpoint the exact rate limiting steps under these conditions.

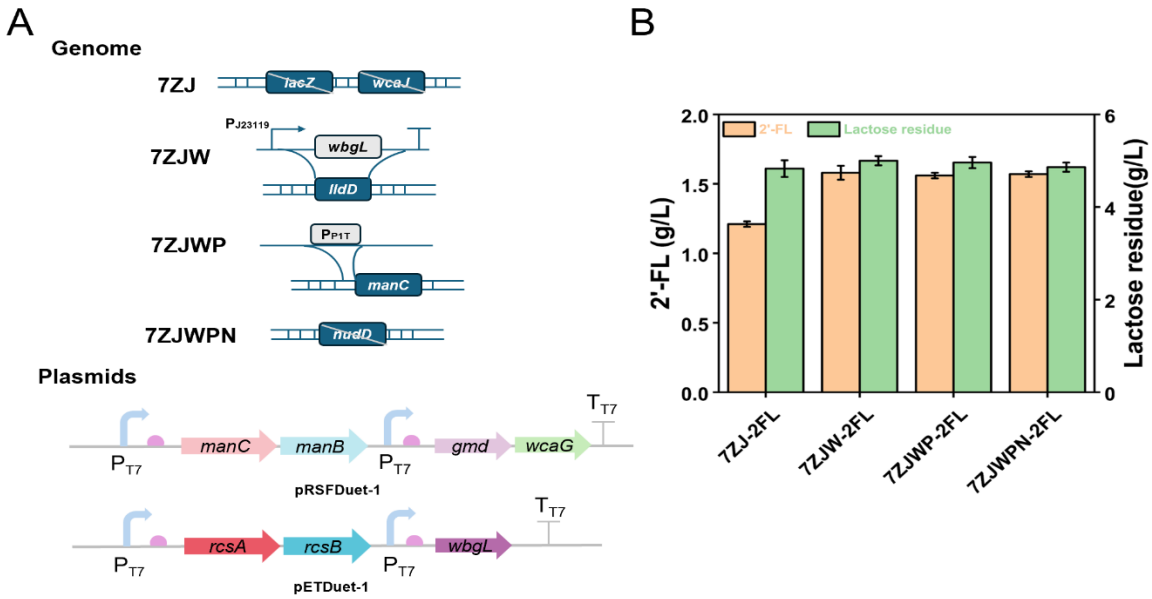

Figure 3. Genome and plasmid interventions evaluated for 2′-FL production. (**A**) Construction of 7ZJ, 7ZJW, 7ZJWP, and 7ZJWPN and organization of pRSF-CBGW and pET-ABW. (**B**) 2′-FL titers and residual lactose for the corresponding production strains.

3.4. Complex Nitrogen Supplementation Enhanced 2′-FL Production

Supplementing a 30 g/L glycerol culture with 5 g/L yeast extract substantially improved both biomass accumulation and 2′-FL production in strain 7ZJW-2FL (Figure 4). Without yeast extract addition, OD_{600} reached a peak 18.08, with 2′-FL concentrations progressing from 2.92 g/L at 24 h to 4.53 g/L at 48 h and 5.03 g/L at 72 h. With yeast extract supplementation, OD_{600} increased to 22.88 at 48 h and 35.28 at 72 h, and 2′-FL titers reached 6.84 g/L at 24 h, 7.71 g/L at 48 h, and 7.50 g/L at 72 h. At the 48 h, the product titer in the supplemented culture was approximately 70% higher than in the control, accompanied by accelerated lactose consumption.

The beneficial impact of yeast extract likely stems from the supply of complex amino acids, vitamins, and nucleosides. These nutrients may boost GTP and NADPH availability, and support overall energy regeneration for the multi enzyme pathway. Crucially, while biomass continued to accumulate between 48 and 72 h, net 2′-FL accumulation plateaued. This identifies 48 h as the optimal operational harvest point, beyond which additional cell growth fails to yield higher recoverable product. These observations suggest that a two stage or controlled fed-batch fermentation strategy, designed to decouple growth from production while maintaining adequate lactose levels, could further optimize process performance.

The value of approximately 7.71 g/L represents a substantial achievement for an EcN shake flask proof of concept. Engineered laboratory strains and alternative hosts can reach higher titers under highly optimized fed batch conditions [12,19–23]. However, cross study comparisons are frequently confounded by host background, vessel scale, carbon source, analytical methods, and sampling time. The defensible conclusion here is that EcN is highly responsive to process improvement, establishing its viability as an alternative manufacturing chassis.

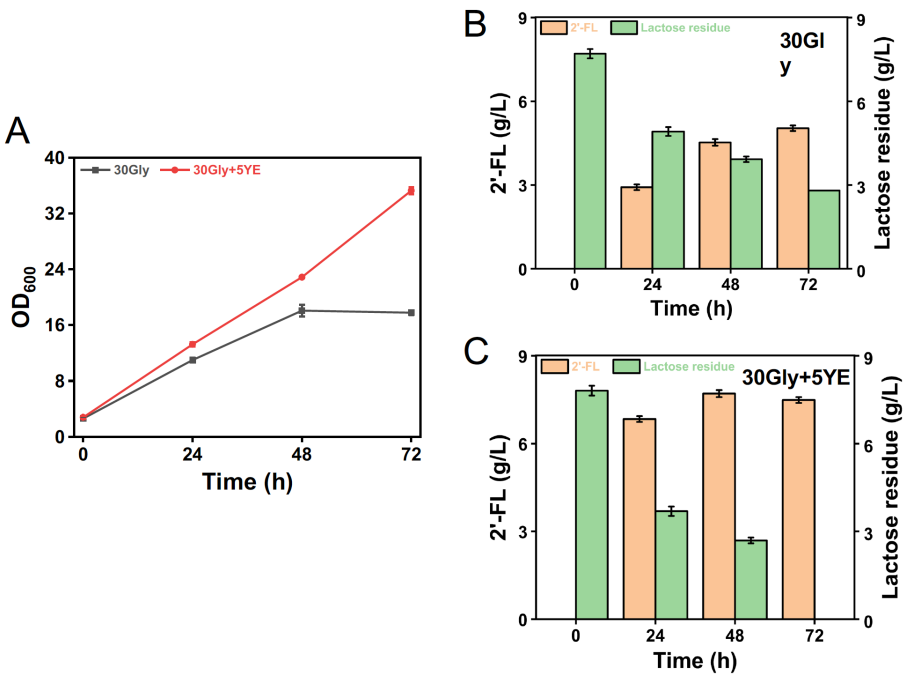

Figure 4. Effect of yeast extract on 2′-FL production by 7ZJW-2FL with 30 g/L glycerol. (**A**) Cell growth without yeast extract (30Gly) or with 5 g/L yeast extract (30Gly + 5YE). (**B**) 2′-FL and residual lactose without yeast extract. (**C**) 2′-FL and residual lactose with yeast extract.

3.5. 3-FL Production Displayed Divergent Responses to Complex Nutrient Addition

Substituting FutM2 for WbgL yielded strain 7ZJ-3FL, which retains the parental 7ZJ genetic background and the pRSF-CBGW donor plasmid (Figure 5A). Without yeast extract addition, 3-FL accumulated steadily, reaching approximately 0.24, 0.34, and 0.38 g/L at 24 h, 48 h, and 72 h, respectively. Unexpectedly, supplementation with 5 g/L yeast extract suppressed 3-FL production despite promoting cell growth. Under supplemented conditions, 3-FL titers reached only 0.07, 0.20, and 0.15 g/L at corresponding time points, representing a 60% reduction at 72 h relative to the control.

This divergent response highlights fundamental biosynthetic and physiological distinctions between the two isomer pathways. Although both strains share an identical host background and donor plasmid, this shared design does not definitively prove that upstream donor supply is nonlimiting in the 3-FL producing strain. We hypothesize that several distinct mechanisms could drive this efficiency gap. First, the kinetic efficiency and substrate affinity toward lactose differ substantially between the two glycosyltransferases. Bacterial α1,3-fucosyltransferases typically exhibit significantly lower catalytic turnover and poorer substrate affinity compared to well established alpha 1,2 fucosyltransferases [16,18,20]. Second, heterologous α1,3-fucosyltransferases are prone to misfolding and inclusion body formation during overexpression in *E. coli*, which restricts the pool of active enzyme [17,19]. Third, nutrient supplementation with yeast extract promotes rapid cell division, which likely aggravates the translational burden and aggregation of FutM2 while channeling central metabolites toward cellular biomass rather than terminal fucosylation. Direct measurements of intracellular donor availability, along with cofactor pools and soluble enzyme fractions, are required to fully distinguish these testable possibilities.

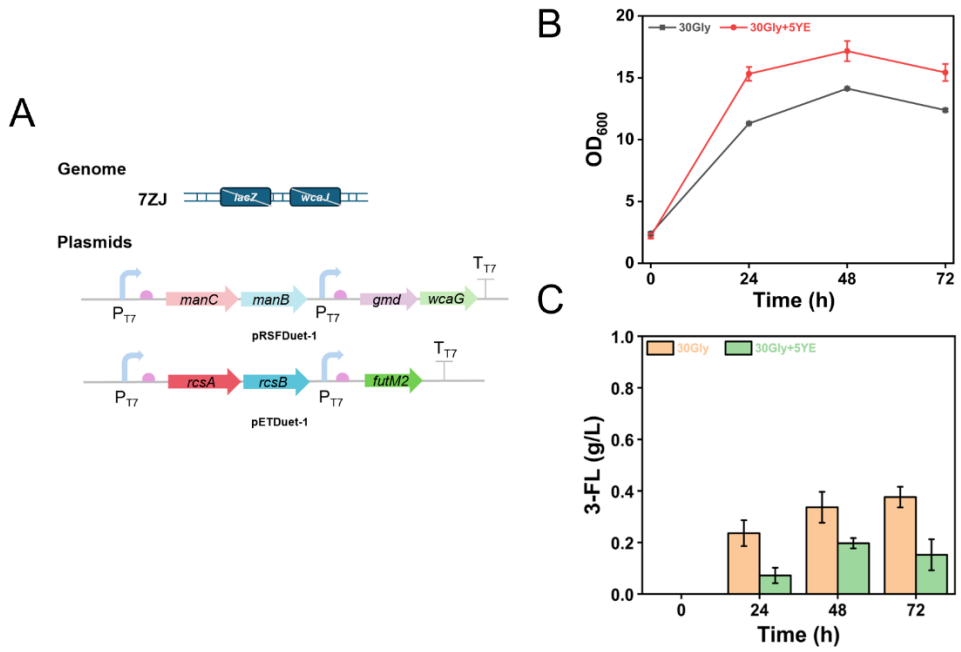

Figure 5. Construction and cultivation response of the 3-FL-producing strain. (**A**) 7ZJ-3FL carried pRSF-CBGW and pET-ABF, with FutM2 replacing WbgL as the terminal fucosyltransferase. (**B**) Growth with 30 g/L glycerol without or with 5 g/L yeast extract. (**C**) 3-FL accumulation under the two conditions.

3.6. Engineering Significance, System Limitations, and Future Priorities

Conventional *E. coli* strains have been extensively optimized for high-titer HMO production, whereas *C. glutamicum* and *B. subtilis* provide robust alternative production backgrounds [6,7,12,16,21,23]. Accordingly, EcN is not positioned here primarily as a chassis for maximizing shake flask titer. Its distinguishing value lies in combining complex HMO biosynthesis with a well characterized probiotic background [24,27,28]. Any future host associated application nevertheless, remains strictly conditional on resolving intestinal substrate availability. In this context, the present study establishes a controlled dual product platform and reveals product specific responses to metabolic interventions, solely validating in vitro production capacity. Because the engineered pathway relies entirely on exogenous lactose and a sufficient carbon supply, intestinal fucosyllactose production cannot be inferred from the present culture experiments. Practical gut deployment would require demonstrating adequate in vivo substrate availability or providing a compatible substrate delivery strategy.

4. Conclusions

This study demonstrates the functional expression of a complete *de novo* GDP-L-fucose pathway in *E. coli* Nissle 1917, enabling the targeted synthesis of both 2′-FL and 3-FL through pairing with WbgL or FutM2. Increasing *wbgL* gene dosage improved 2′-FL accumulation, while nutrient supplementation with yeast extract enhanced 2′-FL titers to approximately 7.71 g/L but significantly reduced 3-FL production. These contrasting outcomes demonstrate that closely related fucosyllactose systems require individualized process optimization. Overall, this work establishes EcN as a feasible in vitro chassis for the production of fucosyllactose under defined culture conditions. Although its distinct probiotic background differentiates this host from conventional production strains, translating this platform toward therapeutic application will strictly depend on resolving intestinal substrate availability, ensuring genetic stability, and implementing rigorous biocontainment.

Supplementary Materials

The following supporting information can be found at: https://www.sciepublish.com/article/pii/1228, Table S1: Oligonucleotides used for gene inactivation; Table S2: Oligonucleotides used for plasmid construction.

Statement of the Use of Generative AI and AI-Assisted Technologies in the Writing Process

During the preparation of this manuscript, the authors used DeepSeek to assist with English-language organization and consistency checking. The authors reviewed and edited the content, verified the scientific claims and references, and take full responsibility for the final published article.

Author Contributions

Conceptualization, Z.-J.L., H.-Z.S. and W.Z.; Methodology, M.-R.W., H.-Z.S., W.Z. and Y.-R.X.; Validation, M.-R.W. and F.-Q.S.; Formal Analysis, M.-R.W.; Investigation, M.-R.W. and F.-Q.S.; Writing—Original Draft Preparation, M.-R.W. and Z.-J.L.; Writing—Review and Editing, Z.-J.L.; Supervision, Z.-J.L.

Ethics Statement

Not applicable. This study did not involve humans or animals.

Informed Consent Statement

Not applicable.

Data Availability Statement

The data supporting the findings of this study are available from the corresponding author upon reasonable request.

Funding

This work was supported by a grant from Deep Sea Biology (Shenzhen) Co., Ltd.

Declaration of Competing Interest

The authors declare that they have no known competing financial interests or personal relationships that could have appeared to influence the work reported in this paper.

References

1. Ballard O, Morrow AL. Human milk composition. *Pediatr. Clin. N. Am.* **2013**, *60*, 49–74. DOI:10.1016/j.pcl.2012.10.002
2. Bode L. The functional biology of human milk oligosaccharides. *Early Hum. Dev.* **2015**, *91*, 619–622. DOI:10.1016/j.earlhumdev.2015.09.001
3. Goehring KC, Marriage BJ, Oliver JS, Wilder JA, Barrett EG, Buck RH. Similar to those who are breastfed, infants fed a formula containing 2′-fucosyllactose have lower inflammatory cytokines in a randomized controlled trial. *J. Nutr.* **2016**, *146*, 2559–2566. DOI:10.3945/jn.116.236919
4. Huang D, Yang K, Liu J, Xu Y, Wang Y, Wang R, et al. Metabolic engineering of *Escherichia coli* for the production of 2′-fucosyllactose and 3-fucosyllactose through modular pathway enhancement. *Metab. Eng.* **2017**, *41*, 23–38. DOI:10.1016/j.ymben.2017.03.001
5. Barnum CR, Paviani B, Couture G, Masarweh C, Chen Y, Huang YP, et al. Engineered plants provide a photosynthetic platform for the production of diverse human milk oligosaccharides. *Nat. Food* **2024**, *5*, 480–490. DOI:10.1038/s43016-024-00996-x

6. Lee YG, Jo HY, Lee DH, Yoon JW, Song YH, Kweon DH, et al. De novo biosynthesis of 2′-fucosyllactose by bioengineered *Corynebacterium glutamicum*. *Biotechnol. J.* **2024**, *19*, 2300461. DOI:10.1002/biot.202300461
7. Zhang Q, Xu X, Zhang W, Huang Z, Wu Y, Liu Y, et al. De novo 2′-fucosyllactose biosynthesis using glucose as the sole carbon source by multiple engineered *Bacillus subtilis*. *Metab. Eng.* **2025**, *88*, 85–93. DOI:10.1016/j.ymben.2024.12.004
8. Wang H, Zhang H, Zhang Z, Chen X, Lai X. Advances in the biosynthesis and application of sialyllactose. *Synth. Biol. Eng.* **2025**, *3*, 10019. DOI:10.70322/sbe.2025.10019
9. Chin YW, Kim JY, Lee WH, Seo JH. Enhanced production of 2′-fucosyllactose in engineered *Escherichia coli* BL21star(DE3) by modulation of lactose metabolism and fucosyltransferase. *J. Biotechnol.* **2015**, *210*, 107–115. DOI:10.1016/j.jbiotec.2015.06.431
10. Li W, Zhu Y, Wan L, Guang C, Mu W. Pathway optimization of 2′-fucosyllactose production in engineered *Escherichia coli*. *J. Agric. Food Chem.* **2021**, *69*, 1567–1577. DOI:10.1021/acs.jafc.0c07224
11. Lin L, Gong M, Liu Y, Li J, Lv X, Du G, et al. Combinatorial metabolic engineering of *Escherichia coli* for de novo production of 2′-fucosyllactose. *Bioresour. Technol.* **2022**, *351*, 126949. DOI:10.1016/j.biortech.2022.126949
12. Liu Y, Zhu Y, Wan L, Chen R, Zhang W, Mu W. High-level de novo biosynthesis of 2′-fucosyllactose by metabolically engineered *Escherichia coli*. *J. Agric. Food Chem.* **2022**, *70*, 9017–9025. DOI:10.1021/acs.jafc.2c02484
13. Chen Y, Zhu Y, Wang H, Chen R, Liu Y, Zhang W, et al. De novo biosynthesis of 2′-fucosyllactose in a metabolically engineered *Escherichia coli* using a novel α1,2-fucosyltransferase from *Azospirillum lipoferum*. *Bioresour. Technol.* **2023**, *374*, 128818. DOI:10.1016/j.biortech.2023.128818
14. Chen R, Zhu Y, Wang H, Liu Y, Meng J, Chen Y, et al. Engineering *Escherichia coli* MG1655 for highly efficient biosynthesis of 2′-fucosyllactose by de novo GDP-fucose pathway. *J. Agric. Food Chem.* **2023**, *71*, 14678–14686. DOI:10.1021/acs.jafc.3c05052
15. Liang S, He Z, Liu D, Yang S, Yan Q, Jiang Z. Construction of an engineered *Escherichia coli* for effective synthesis of 2′-fucosyllactose via the salvage pathway. *Synth. Syst. Biotechnol.* **2024**, *9*, 108–114. DOI:10.1016/j.synbio.2024.01.001
16. Li M, Li C, Luo Y, Hu M, Liu Z, Zhang T. Multi-level metabolic engineering of *Escherichia coli* for high-titer biosynthesis of 2′-fucosyllactose and 3-fucosyllactose. *Microb. Biotechnol.* **2022**, *15*, 2970–2981. DOI:10.1111/1751-7915.14152
17. Chen G, Wu H, Zhu Y, Wan L, Zhang W, Mu W. Glycosyltransferase from *Bacteroides gallinaceum* is a novel α-1,3-fucosyltransferase that can be used for 3-fucosyllactose production in vivo by metabolically engineered *Escherichia coli*. *J. Agric. Food Chem.* **2022**, *70*, 1934–1942. DOI:10.1021/acs.jafc.1c06719
18. Yu J, Shin J, Park M, Seydametova E, Jung SM, Seo JH, et al. Engineering of α-1,3-fucosyltransferases for production of 3-fucosyllactose in *Escherichia coli*. *Metab. Eng.* **2018**, *48*, 269–278. DOI:10.1016/j.ymben.2018.05.021
19. Chen Y, Zhu Y, Wang H, Chen R, Du Z, Mu W. Efficient production of 3-fucosyllactose in a plasmid-free engineered *Escherichia coli* through strengthening of the GDP-fucose pathway. *Food Biosci.* **2024**, *59*, 104154. DOI:10.1016/j.fbio.2024.104154
20. Jia R, Li M, Miao M, Zhang T. Efficient de novo synthesis of 3-fucosyllactose in *Escherichia coli* via enzyme engineering and pathway refinement. *Bioresour. Technol.* **2025**, *436*, 132974. DOI:10.1016/j.biortech.2025.132974
21. Li N, Yan S, Xia H, Fang Y, Niu K, Li G, et al. Metabolic engineering of *Escherichia coli* BL21(DE3) for 2′-fucosyllactose synthesis in a higher productivity. *ACS Synth. Biol.* **2025**, *14*, 441–452. DOI:10.1021/acssynbio.4c00598
22. Zhang K, Gao M, Cao C, Zhang M, Ahmad W, Rady A, et al. Intensification of 2′-Fucosyllactose biosynthesis pathway by using a novel fucosyltransferase from Bacillus cereus. *Front. Bioeng. Biotechnol.* **2025**, *13*, 1569597. DOI:10.3389/fbioe.2025.1569597
23. Zhu Y, Zhao M, Wang H, Zhu Y, Mu W. Metabolic engineering of *Escherichia coli* BL21(DE3) cocultured with glucose and xylose for efficient production of 2′-fucosyllactose. *Bioresour. Technol.* **2025**, *419*, 132062. DOI:10.1016/j.biortech.2025.132062
24. Sonnenborn U. *Escherichia coli* strain Nissle 1917—from bench to bedside and back: history of a special *Escherichia coli* strain with probiotic properties. *FEMS Microbiol. Lett.* **2016**, *363*, fnw212. DOI:10.1093/femsle/fnw212
25. Cress BF, Linhardt RJ, Koffas MAG. Draft genome sequence of *Escherichia coli* strain Nissle 1917 (serovar O6:K5:H1). *Genome Announc.* **2013**, *1*, e00047-13. DOI:10.1128/genomeA.00047-13
26. Revelles O, Millard P, Nougayrède JP, Dobrindt U, Oswald E, Létisse F, et al. The carbon storage regulator (Csr) system exerts a nutrient-specific control over central metabolism in *Escherichia coli* strain Nissle 1917. *PLoS ONE* **2013**, *8*, e66386. DOI:10.1371/journal.pone.0066386
27. Riglar DT, Giessen TW, Baym M, Kerns SJ, Niederhuber MJ, Bronson RT, et al. Engineered bacteria can function in the mammalian gut long-term as live diagnostics of inflammation. *Nat. Biotechnol.* **2017**, *35*, 653–658. DOI:10.1038/nbt.3879
28. Isabella VM, Ha BN, Castillo MJ, Lubkowicz DJ, Rowe SE, Millet YA, et al. Development of a synthetic live bacterial therapeutic for the human metabolic disease phenylketonuria. *Nat. Biotechnol.* **2018**, *36*, 857–864. DOI:10.1038/nbt.4222

29. Yu X, Guo J, Sun J, Zhang C. Navigable genome engineering: Stepwise correlation for precision-guided optimization of microbial cell factory phenotypes. *Synth. Biol. Eng.* **2025**, *3*, 10003. DOI:10.70322/sbe.2025.10003
30. Gan M, Chen C. Synthetic biology-inspired biocontainment strategies of therapeutic genetically engineered bacteria. *Synth. Biol. Eng.* **2026**, *4*, 10001. DOI:10.70322/sbe.2026.10001
31. Shao F, Wu R, Li ZJ. Metabolic engineering of *Escherichia coli* Nissle 1917 for the production of heparosan using mixed carbon sources. *Fermentation* **2025**, *11*, 289. DOI:10.3390/fermentation11050289
32. Fu XZ, Tan D, Aibaidula G, Wu Q, Chen JC, Chen GQ. Development of *Halomonas* TD01 as a host for open production of chemicals. *Metab. Eng.* **2014**, *23*, 78–91. DOI:10.1016/j.ymben.2014.02.006
33. Wang MR, Tao S, Lin N, Song X, Li ZJ. Development of *Photobacterium* sp. LN01 as a versatile halophilic platform for tunable biosynthesis of polyhydroxyalkanoates. *ACS Synth. Biol.* **2025**, *14*, 4090–4099. DOI:10.1021/acssynbio.5c00562